AJSTD Vol. 26 Issue 2 pp. 73-84 (2010)

MEASURMENT OF BENDING PROPERTIES OF RHIZOPHORA TROPICAL WOOD

Sinin Hamdan*[a], Mahbub Hasan[b] and Yoann Nohe[c]

[a]Faculty of Engineering, Universiti Malaysia Sarawak, 94300 Kota Samarahan, Sarawak, Malaysia
[b]Department of Materials & Metallurgical Engineering, Bangladesh University of Engineering & Technology, Dhaka, Bangladesh
[c]University of Technology Belfort Montbeliard (UTBM), 90010 Belfort Cedex, France

* Corresponding Author: Sinin Hamdan, E-mail: hsinin@feng.unimas.my,
Tel: +60-82-583232, Fax: +60-82-583410

ABSTRACT

The Young's modulus, load at the yield point and proportional limit stress from the compression bending (cb) test were compared with the four point bending tests (4pb). The theoretical Young's modulus are larger than the real reading for 5mm and 10mm thick specimens, except for 200mm long specimens due to specimen nonlinearity. The experimental results for the short specimens are slightly high compared to the theory due to uniaxial compression in both tensile and compressive planes. Since the additional deflection produced by the shearing force and the stress concentration at the loading point was smaller with the compression bending test compared to the conventional four point bending test the values of E_{cb} are larger than E_{4pb}. It is noted that when length/thickness (l/t)>80, the values of E_{cb} are scattered. In addition, E_{cb} decrease sharply when l/t<30. In order to obtain a stable Young's modulus value, it is suggested that the l/t should be 30~80.

Keywords: Young's Modulus; Proportional Limit Stress; Compression Bending Test; Four Point Bending Test; Length to Thickness Ratio

1. INTRODUCTION

Bakau (Rhizophora) is a common mangrove tree from Rhizophorace family. It grows best in wet, muddy and salty sediments. Bakau can be immediately recognized by its arching prop and stilt roots. Bakau wood is used extensively in Borneo and South East Asia for the piling of small building and to support small box culvert. Bakau pile is also used in order to reinforce the ground below a raft or footing for a small building. However Bakau pile had never been studied from a mechanical point of view. Previous studies on the bending test method for wood suggest that the stress condition around the loading nose is distorted seriously and that the bending properties are influenced by the loading condition. A compression bending test method based on buckling has been proposed previously. This method of testing corresponds with the traditional use of Bakau wood as pile and removes the undesirable stress concentration from the typical loading nose of the conventional three or four point bending test. In current study, the Young's modulus from the compression bending (cb) test (E_{cb}) and proportional limit stress (σ_{pl}) by the compression bending test were examined and the applicability of the testing method were compared to the conventional bending test methods.

2. THEORY

In engineering mechanics, bending (also known as flexure) characterizes the behavior of a structural element subjected to a lateral load. A structural element subjected to bending is known as a beam. Bending produces reactive forces inside a beam as the beam attempts to accommodate the flexural load. Beam bending is analyzed with the Euler-Bernoulli beam equation. The classic formula for determining the bending stress in a member is;

$$\sigma=My/I_x \quad (1)$$

Where σ is the bending stress, M is the moment at the neutral axis, y is the perpendicular distance to the neutral axis, I_x is the second moment of inertia about the neutral axis x.

Equation (1) can be simplified to;

$$\sigma=6M/bt^2 \quad (2)$$

where b is the width of the section being analyzed and t is the thickness. Equation (2) is valid only when the stress at the extreme fiber (the portion of the beam furthest from the neutral axis) is below the yield stress of the material. At higher loadings the stress distribution becomes non-linear and ductile materials will eventually enter a plastic state where the magnitude of the stress is equal to the yield stress everywhere in the beam, with a discontinuity at the neutral axis where the stress changes from tensile to compressive. Figure 1 show the schematic diagram of compression bending test.

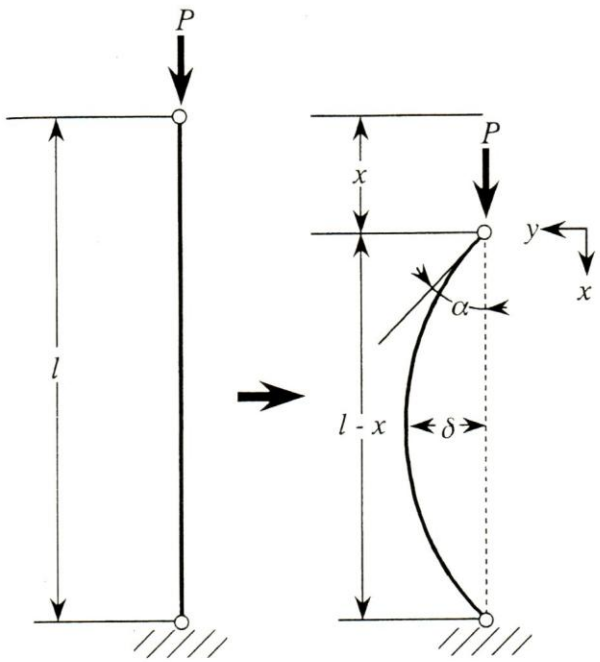

Figure 1: Schematic diagram of compression bending

When axial load P is applied in the long axis and δ_A is the deflection at the mid-span A, the bending moment at the mid-span is given by;

$$M_A=P\delta_A \quad (3)$$

From equation (2), σ can be derived when the deflection δ_A is measured. When the loading point displaces x after bifurcation, x/l (where l is the length) is derived by the following equation;[1]

$$x/l=2-[2E(p)/k(p)] \quad (4)$$

Where p is represented by the deflection angle at loading point α;

$$p=\sin(\alpha/2) \quad (5)$$

$$E(p) = \int_0^{\frac{\pi}{2}} \sqrt{1 - p^2 \sin^2 \varphi} d\varphi \quad (6)$$

$$\text{and } k(p) = \int_0^{\frac{\pi}{2}} \frac{d\phi}{\sqrt{1 - p^2 \sin^2 \phi}} \quad (7)$$

A method for determining ρ, the radius of curvature at the mid-span is to measure the strains at the outer planes. When the tensile and compressive strains at the outer planes are ε_t and ε_c respectively, ρ is obtained as;

$$\rho = t/(\varepsilon_t - \varepsilon_c) \quad (8)$$

The radius of the curvature ρ can also be obtained by p and K(p);

$$\rho/l = 1/4pK(p) \quad (9)$$

The longitudinal strain at the outer plane ε is determined by the following two procedures. From equations (4) and (9), the ρ/l and x/l relation is derived by intervening the angle α, as shown in Figure 2. Then ε_1 is derived by the radius of curvature as;

$$\varepsilon_1 = t/2\rho \quad (10)$$

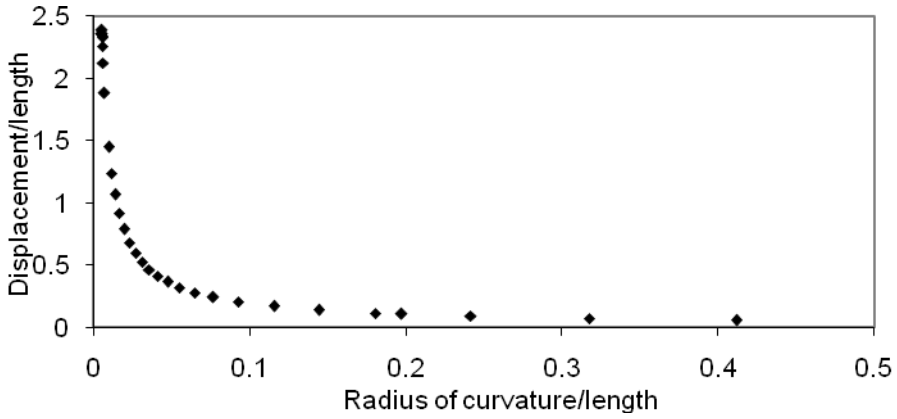

Figure 2: The displacement/length versus radius of curvature/length at the midspan.

Another method is to average the absolute values of tensile and compressive strains from direct reading of strain gauges. By this method, ε_2 is derived as;

$$\varepsilon_2 = (|\varepsilon_t| + |\varepsilon_c|)/2 \quad (11)$$

The σ-ε relation can be plotted by these procedures and then the Young's modulus can be determined. When determining the relation between ρ/l and x/l (Figure 2), this relation is approximated by a power function before and after x/l = 0.1;

$$\rho/l = 0.101(x/l)^{-0.5} \qquad 0 \leq x/l < 0.1 \quad (12a)$$

$$\rho/l = 0.138(x/l)^{-0.56} \qquad x/l \geq 0.1 \quad (12b)$$

3. MATERIALS AND METHODS

Specimens with various length to thickness ratios were cut from Rhizophora tropical wood having rectangular cross sections of 5mm/10mm/15mm (radial direction) x 25mm (tangential direction). The lengths were varied in the range of 200-500mm at an interval of 100mm. Six specimens were used in each test condition. A Shimadzu AG-IS MS series Autograph universal testing machine (Figure 3) was used for conducting the test. The deflection at the mid-span (δ_A) was measured with a linear voltage displacement transducer (LVDT) connected to an oscilloscope (Picoscope). Strain gauges were bonded at the center of the longitudinal-tangential planes of each size of the specimen for measuring normal strains in the loading direction, ε_t and ε_c. The measurement of the strain was recorded with a Vishay P3 strain recorder and indicator. These data were used for real measurement.

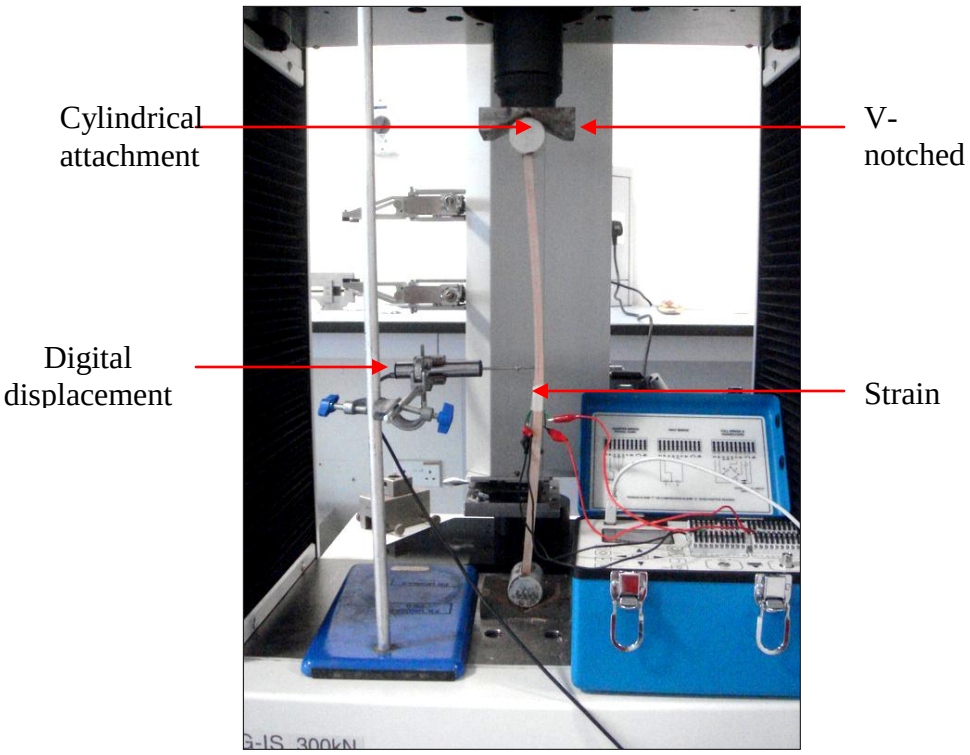

Figure 3: Compression bending test equipment.

The specimen whose sides were inserted into the grooves cut on the sides of cylindrical attachments was supported between the V notches. The load was applied by means of these attachments that rotate freely in the V notches. The load was applied axially at 0.5mm/minute and the loading point displacement was measured from the cross-head movement. The E and σ_{pl} were obtained from the load, the loading point displacement, the strains at the outer surfaces and the deflection until the yield point.

Three tests with strain gauges were conducted in order to prove the validity of equation (10). From the relations between ρ/l and x/l, the σ-ε relation was obtained by the procedure

mentioned above. This σ-ε relation was regressed into the Ramberg-Osgood's power function. The Ramberg-Osgood equation[2] was created to describe the non linear σ-ε relationship near their yield points;

$$\varepsilon=\sigma/E+k(\sigma/E)^n \quad (13)$$

Where k and n are constants that depend on the material. The first term on the right side, σ/E, is equal to the elastic part of the strain, while the second term, $k(\sigma/E)^n$, accounts for the plastic part with the parameters k and n describing the hardening behavior of the material. Introducing the yield strength of the material, σ_o and defining a new parameter, α, related to k as $\alpha=k(\sigma_o/E)^{n-1}$, it is convenient to rewrite the term on the extreme right side as follows;

$$k(\sigma/E)^n=\alpha\sigma_o/E(\sigma/\sigma_o)^n \quad (14)$$

Replacing in the first expression, the Ramberg-Osgood equation can be written as:

$$\varepsilon=\sigma/E+\alpha\sigma_o/E(\sigma/\sigma_o)^n \quad (15)$$

The value $\alpha=\sigma_o/E$ can be seen as a yield offset. This comes from the fact that;

$$\varepsilon=(1+\alpha)\sigma_o/E \quad (16)$$

when $\sigma=\sigma_o$ (17)

Elastic strain at yield $=\sigma_o/E$ (18)

and

Plastic strain at yield $= \alpha(\sigma_o/E)\sigma$ = yield offset (19)

The compression bending test was compared to the conventional four point bending test and the bending properties was measured by elementary bending theory. The dimensions of the four point bending test beams were 15mm in width, 15mm in thickness and 600mm in length. The beam was supported by a span of 450mm and the load was vertically applied at the trisected points by loading nose whose radii was 10mm. The loading velocity was 1mm/minute and the deflection at the center of the specimen was measured by a LVDT placed below the specimen. There exist a constant linear relation between the loading displacement x and the deflection measured with the LVDT (δ_A) that is;

$$\delta_A=1.05x-0.06 \quad (20)$$

Three tests were conducted to determine this relation (equation (20)) and the loading displacement x was used instead of the digital LVDT (δ_A) for the experiment. Strain gauges were also bonded to similar specimens for real measurements. The load, loading point displacement and strain at the center were measured simultaneously. The load-deflection, load-loading point displacement and load-strain_relations were regressed into the Ramberg-Osgood's function. The E and σ_{pl} were calculated by substituting the parameters obtained by the regression into the equations derived from elementary bending theory (bt);

$$E_{bt}=23L^3\Delta P/108wh^3\Delta y \quad (21)$$

$$\sigma_{bt}=P_{bt}/wh^2 \quad (22)$$

Where L, w and h are the span length, breadth and depth of the specimen respectively. Six specimens were used for the four point bending tests.

4. RESULTS AND DISCUSSION

4.1 Direct Reading with Strain Gauges and Theoretical Calculations

Figures 4 to 6 show the E_{cb} obtained using the strain gauges from the compression bending test. The light columns show the theoretical E_{cb} obtained using equation (11) that is $\varepsilon_2=[\,|\varepsilon_t|+|\varepsilon_c|\,]/2$ and using the theoretical relation between ρ/l and x/l (Figure 1). The shaded columns show the E_{cb} obtained from equation (10) and direct reading of the strain gauges and LVDT. It is found that the theoretical E_{cb} are larger than the real reading for specimens with a thickness of 5mm and 10mm, except for the specimens with a length of 200mm. It is noticed that for short specimens (200mm) the experimental results are higher compared to the theoretical results. The fact that the theory yields higher values than the real readings can be explained by the non linearity in material like wood, where weakness are likely to exist in long specimen. Indeed, the theory is for perfect specimens.

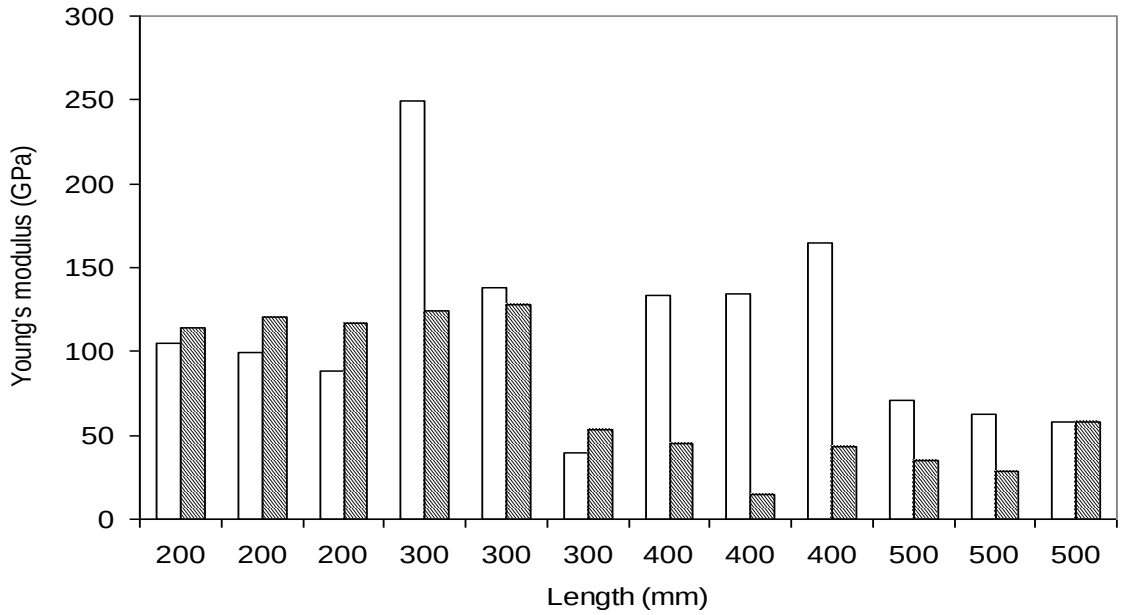

Figure 4: Young's modulus corresponding to the length with a thickness of 5mm and width of 25mm obtained from the strain gauges. Light and shaded represent theoretical and experimental results respectively.

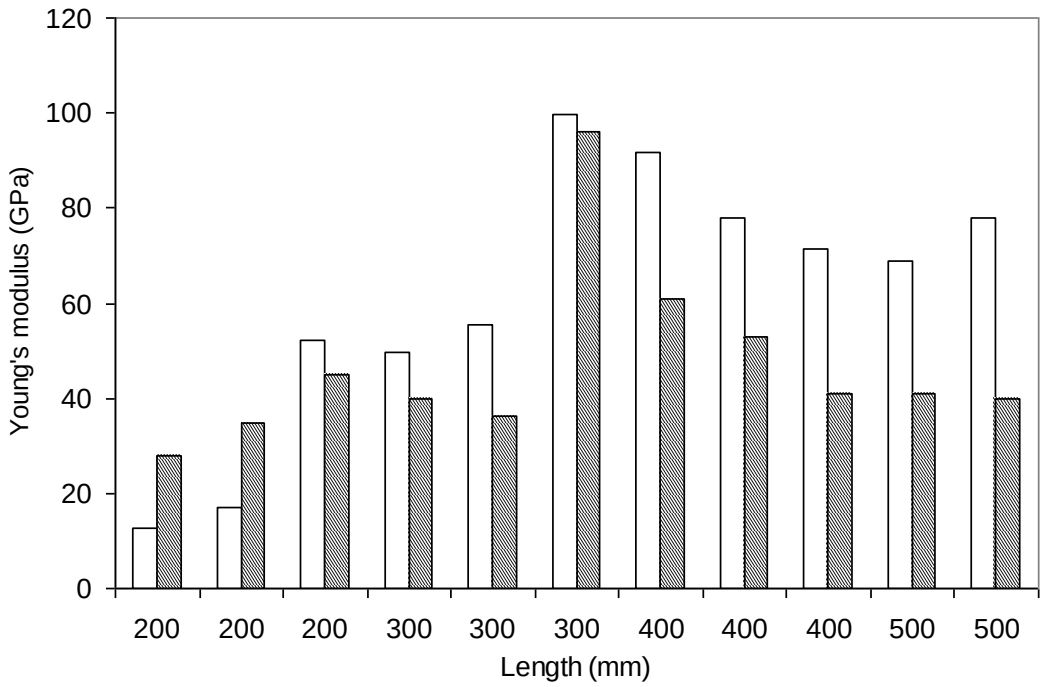

Figure 5: Young's modulus corresponding to the length with a thickness of 10mm and width of 25mm obtained from the strain gauges. Light and shaded represent theoretical and experimental results respectively.

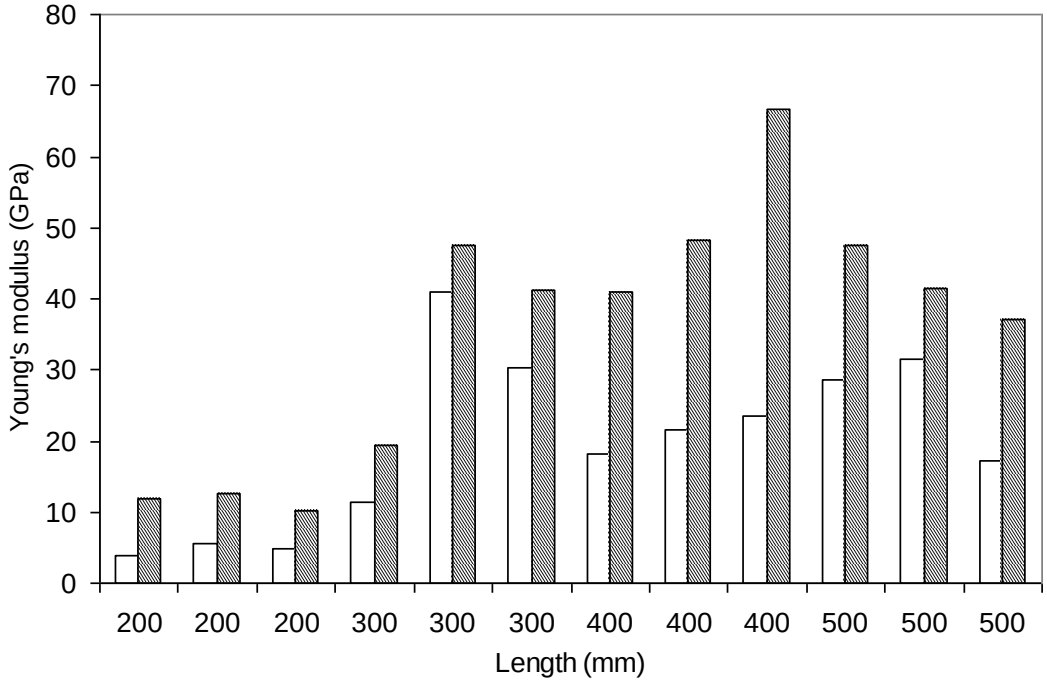

Figure 6: Young's modulus corresponding to the length with a thickness of 15mm and width of 25mm obtained from the strain gauges. Light and shaded represent theoretical and experimental results respectively.

Figures 7 and 8 are the readings of the strain gauges for specimens of 10mm x 25mm x 200mm and 10mm x 25mm x 500mm respectively. It is noticed that for the short specimen the ε_t at the outer planes is also negative like the ε_c. This is due to the short length where both planes experienced uniaxial compression**.** On the other hand, the readings of the strain gauges from the long specimens diverge sharply where the tensile planes experienced purely tension. The bending was not significant with short specimens (200mm) since uniaxial compression are more significant rather than compression bending. Moreover for the 15mm thick specimens, the Young's modulus from the strain gauges are all higher than the theoretical results. For this reason only the specimens with a thickness of 5mm and 10mm are analyzed.

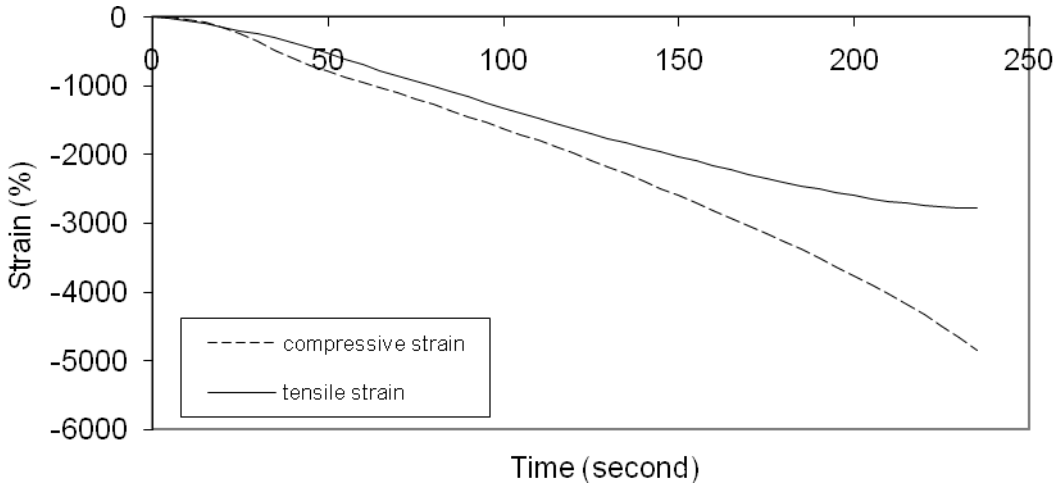

Figure 7: Readings of the tensile and compressive strain (ε_t, ε_c) from strains gauges for a specimen of 10mm x 25mm x200mm.

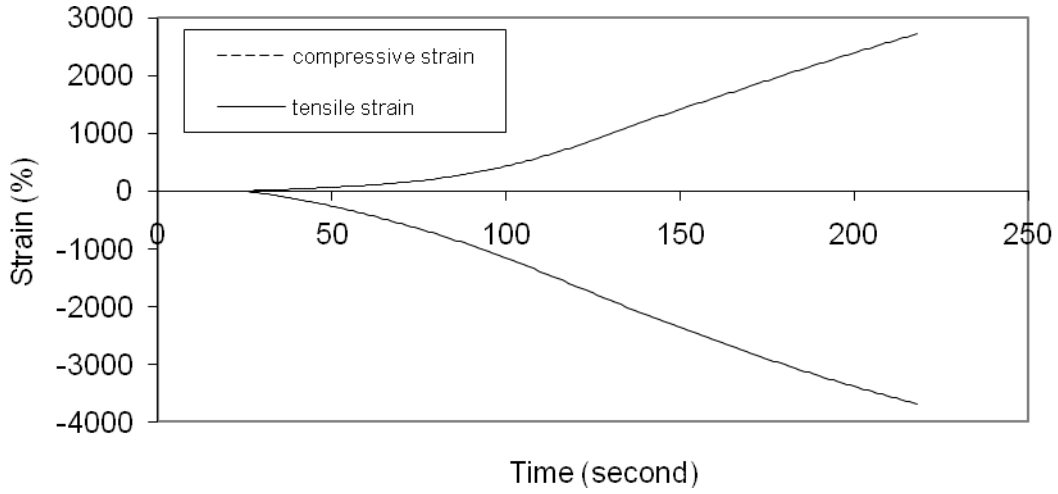

Figure 8: Readings of the tensile and compressive strain (ε_t, ε_c) from strains gauges for a specimen of 10mm x 25mm x 500mm.

4.2 Young's Modulus Corresponding to Length/Thickness

Figure 9 shows the average E_{cb} corresponding to the l/t obtained by the compression bending tests of the specimens whose thickness were 5mm and 10mm with the standard deviations. The average value for six specimens obtained from the four point bending test is 18GPa. The values of E_{cb} are larger than E_{4pb}. It is suggested that the additional deflection produced by the shearing force and the stress concentration at the loading point was smaller with the compression bending test compared to the conventional bending test. Furthermore the loading nose dimension for the four point bending test was definitively too small that is the diameter was only 10mm. In order to have a better representation of the shearing force and the stress concentration, it is thought that the use of larger radii of the loading nose is more appropriate.[3] It is noted that when l/t >80, the values of E_{cb} are scattered. This is attributed to the material non linearity. In addition, E_{cb} decrease sharply when l/t <30 and this is thought to be due to the geometrical effect. As seen previously, the short specimens react in uniaxial compression rather than compression bending. Although the shearing force are less compared with the conventional four point bending test, it cannot be entirely eliminated and is significant when l/t is small. In order to obtain a stable Young's modulus value, it is suggested that the l/t should be 30~80.

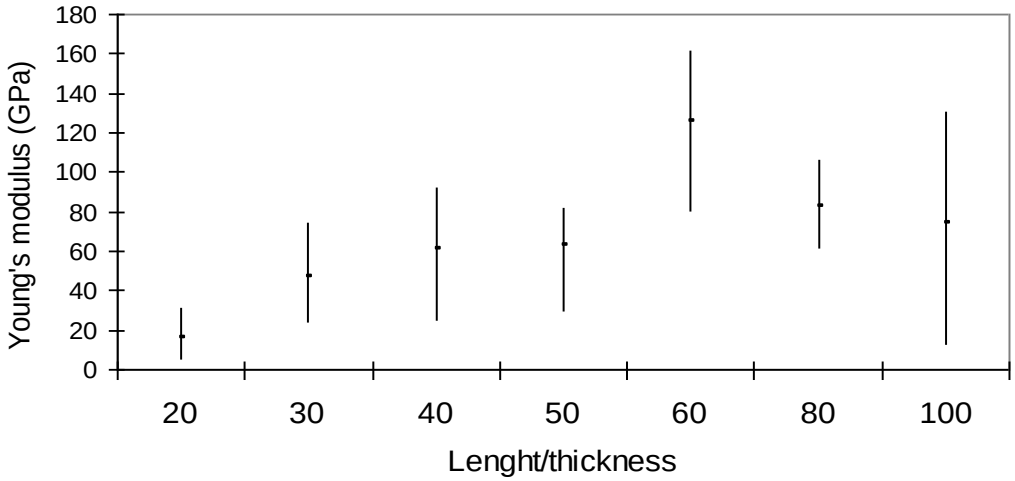

Figure 9: Young's Modulus corresponding to the length/thickness.

4.3 Proportional Limit Stress Corresponding to the Lentgh/Thickness

Figure 10 shows the σ_{pl} corresponding to the various l/t. The values of σ_{pl} increase gradually until it reach beyond the average value obtained from the four point bending test and it decrease after l/t=60. This l/t =60 value is considered as an optimum. From Figure 8 it is suggested that σ_{pl} at l/t <60 are influenced by the shearing force due to their geometry and σ_{pl} at l/t >60 are influenced by the non linearity of the material.

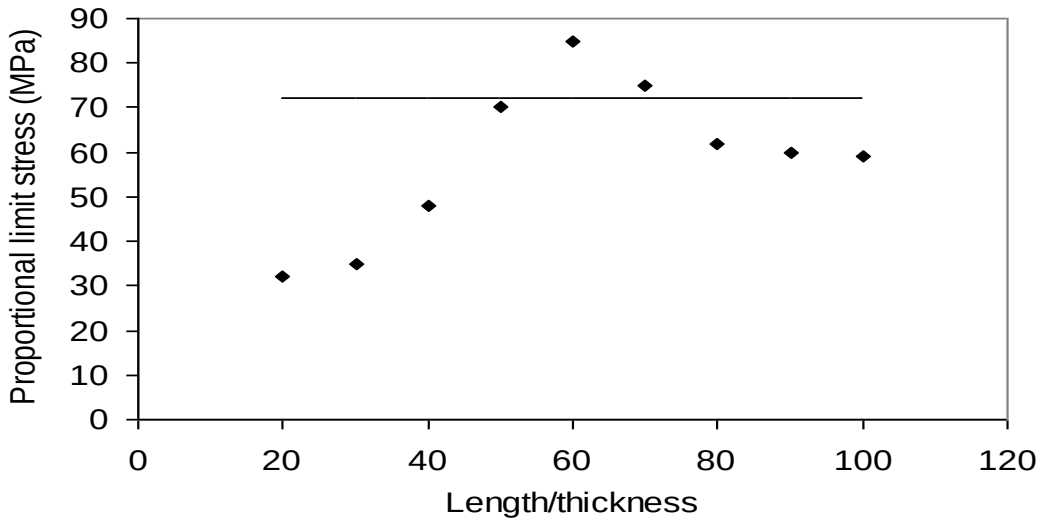

Figure 10: Proportional limit stress corresponding to the length/thickness for specimens whose thickness were 5mm and 10mm. The line represents the average value obtained by the four point bending test.

5. CONCLUSION

In order to obtain the E_{cb} and σ_{pl}, the compression bending test was conducted on Bakau wood columns with various l/t. The validity of the testing method was examined by comparing these results with the conventional four point bending test. It is concluded that compression bending are valid for specimens of lenght >300mm, since in short specimens (<200mm) uniaxial compression occurs rather than compression bending. For thin specimens (t=5mm), E_{cb} reduce with length due to bigger ρ, whereas for intermediate thick specimens (t=10mm), E_{cb} are almost constant for all values of l. For thick specimens (t=15mm), theoretical E_{cb} increase with l which is not true as reflected by the direct reading which showed E_{cb} decrease with l. The bending properties can be obtained by the compression bending test without stress concentration that normally occurs in the conventionnal three or four point bending test methods. It can be concluded that the theory fit very well with medium thick specimens (t=10mm), as an optimum thickness for testing Bakau wood which is also proven by direct reading.

It is noticed that for short specimens (200mm) the experimental results are higher compared to the theoretical resulus. This is due to the fact that the non linearity in wood exist in long specimen and therefore the theory yields higher values than the real reading. The short specimens react in uniaxial compression rather than compression bending where Young's modulus value is 18 when length/thickness is 20. This value is similar for the average value from six specimens obtained from the four point bending test i.e. 18 GPa. A stable Young's modulus value is obtained when length/thickness are between 30~80 and the proportional limit stress from compression bending test fit well with the four point bending test at length/thickness between 50-70.

References

[1] Fukuda, H. and Itabashi, M., *Comp. A*, 1999, 30, 249-256.

[2] Yoshihara, H. and Oka, S., *J. W. Sci.*, 2001, 47, 262-268.

[3] Yoshihara, H. and Fukuda, A., *J. W. Sci.*, 1998, 44, 473-481.